Rotary Machines Fault Diagnosis based on Principal Component Analysis

M. Elsamanty[1,2], W.S. Salman [1,3], , A. A. Ibrahim[1]

[1] Faculty of Engineering at Shoubra, Benha University, 108 Shoubra St., Cairo, Egypt

Mahmoud.alsamanty@feng.bu.edu.eg, wael.saady21@feng.bu.edu.eg, abdelkader.ibrahim@feng.bu.edu.eg

[2] Smart Engineering Systems Research Center (SESC), Nile University, 12588, Shaikh Zayed City, Giza, Egypt

melsamanty@nu.edu.eg

[3] Fayoum University, Faculty of Engineering, Mechanical Department, Fayoum, Egypt

wsa12@fayoum.edu.eg

Abstract

Rotating machines are commonly used in industrial applications. Mechanical faults such as rotor unbalance, shaft misalignment, pulley misalignment, structural looseness, and bearing faults leading to unplanned shutdown based on the severity of these faults. The condition monitoring technique based on vibration analysis has the potential to detect and diagnose a great number of early stage faults. However, some mechanical faults have correlated vibration features leading to ambiguous diagnosis to identify and distinguish these faults. In this paper, a proposed method based on the Principal Component Analysis (PCA) is presented to produce uncorrelated Principal Components (PCs) to identify the healthy and different faulty cases. A test rig was prepared to simulate a group of mechanical faults such as rotor unbalance, pulley misalignment, belt damage, combined unbalance with pulley misalignment, and combined unbalance with belt damage. The conventional vibration measurements were collected for each case and their features were extracted and used to produce the equivalent PCs. It was found that the produced uncorrelated PCs have the superior to distinguish the majority of simulated faults which have correlated vibration features as presented in the rest of paper.

Keywords: Condition Monitoring, Vibration Signatures, Fault Diagnosis, Rotating Machine, Principal Component Analysis

1. Introduction

Rotary machines in general configuration consist of three main parts; rolling or journal bearings (anti-friction or fluid bearings), rotor, and foundation. Since rotary machines commonly work in a tough operating environment, this makes it more expose to different types of faults and increases the difficulty of fault diagnosis. The failure in rotating machines leads to productivity loss, economic, safety, and environmental issues [1]-[4]. Early fault detection is necessary to keep the cost in industry by keeping machine life time and spare parts. Therefore, the advanced maintenance systems move to another form of maintenance handling called predictive maintenance. Predictive maintenance based condition monitoring is employed to improve the productivity rate, production quality, and the efficiency of manufacturing plants. The main concept of predictive maintenance is to achieve early detection of potential failures. In the case of machines driven by induction motor, the predictive maintenance is performed to detect the initial failures due to rotor unbalance, bearing defects, and shaft misalignment. Also, it is employed to detect faults in the induction motors such as stator windings shortage, broken rotor bar(s), and air gap eccentricity. The core benefit of the early fault detection is to prevent the sudden failure due to heat generation from faults and decrease the consumed energy.

More efforts were presented to detect and monitor the different faults initiated in rotary machines based on different condition monitoring methods. Independence-oriented variational mode decomposition method was proposed via correlation analysis to adaptively get the weak and compound fault feature of wheelset bearing[5]. Stochastic resonance was initially investigated in a multi-stable system by computing its output spectral amplification, analyzed its output frequency response numerically, and examined the effect of both rescaling and damping factors on output responses. Finally, a method was presented based on damped stochastic resonance with stable-state matching to initiate bearing fault diagnosis [6]. Multi-speed fault diagnostic approach was presented based on self-adaptive wavelet transform components produced from bearing vibration signals [7]. The presented approach can distinguish between signatures of four conditions of roller bearing, i.e., healthy bearing and three different types of defected bearings on the inner race, outer race, and roller separately. A bearing fault diagnosis technique was developed to increase the diagnosis accuracy [8]. Five features were selected as predictors in multi-class Support Vector Machine (SVM) classification. The five selected features are entropy estimation error, mean, Root Mean Squared (RMS), kurtosis, and histogram lower bound. Multi-fault diagnosis scheme for bearings was presented using hybrid features resulting from their acoustic emissions and a standard multi-class extension of the binary SVM [9]. Complete Ensemble Empirical Mode Decomposition (EEMD) was used with adaptive noise to detect rolling element bearings' faults [10]. The effect of sparse auto-encoder on the ordering performance of significantly compressed measurements of bearing vibration signals was displayed computationally [11]. Principal Component Analysis (PCA) was applied to the features extracted from vibration and current signatures and the artificial neural network and genetic algorithms were employed to classify induction motor faults [12]. It was observed that the performance of fault classification was improved after adding PCA. A method of bearing faults diagnosis was presented based on linear discriminant analysis, neighborhood component analysis, and PCA which achieved good results in dimensionality reduction [13]. PCA, linear discriminant analysis, fisher score, and a genetic algorithm were also applied to estimate an optimized and reduced features from vibration dataset [14]. An experiment was set up to compare health conditions of a motor and determine if their

patterns could be grouped using PCA [15]. The result demonstrated that the proposed method successfully identified healthy, unbalance and parallel misalignments of rotary rotor. Three identical induced draft fans were monitored together using an unsupervised statistical algorithm based on PCA [16]. It was observed that the PCA based technique is a good fit for early fault detection compared to the conventional methods. PCA and empirical mode decomposition method were used to monitor the running states of rolling bearings [17]. The experiment results showed that the whole life cycle of the rolling bearings can be classified into five different operating periods and each period represents a different bearing operating state.

The conventional vibration methods faced an issue when analyzing vibration signals since the features which distinguish healthy and different faulty cases are highly correlated which ultimately can bias the results of the algorithm leading to an ambiguous diagnosis. In this research, an improvement method based on PCA is presented to identify and distinguish different cases since PCA decreases the dimensionality and correlation of these features [18], [19]. Conventional vibration signals were collected and their features were extracted. After that, these features were employed as input parameters to the PCA model. The paper was arranged to define the vibration features and the mathematical model of PCA in section (2). Section (3) describes the rotary machine test rig and definitions for applied mechanical faults. Instrumentation and software are discussed in section 4. Experimental results and analysis are presented in section (5). Finally, section (6) discusses the research conclusions.

2. Analysis Methods

This section presents the concept and mathematical theory of method which has been applied to identify the different mechanical faults as mentioned above. It was classified into two subsections. The first one discusses the features of vibration pattern for different faults and the second one displays how to employ these features to identify the different faults through the PCA.

2.1 Vibration Signatures

The vibration analysis of rotary machine is based on detecting mechanical faults which are associated with the operation and mounting of the machine. Almost of mechanical faults are detected in the low frequency range (0~5X), where X is the machine rotating frequency. For example, rotor unbalance and bent shaft can increase the amplitude at X, shaft misalignment increases the amplitude at X and 2X, external and internal looseness increase the amplitude at X, 2X, …, nX, where n is the harmonic number. Monitoring these components based on the signature of vibration analysis has a considered contribution in detecting these types of faults. In this research the amplitude of the components 1X, 2X, 3X were recorded for different fault cases. In addition, RMS of time signal was estimated.

2.2 Principal Component Analysis

One of the most common problems in the analysis of various data observations is the highly correlated features. The main idea of PCA is to decrease the dimensionality of a data set in which there are a large number of related variables, while retaining as much as possible of the variation present in the data set. This reduction is achieved by transforming to a new set of variables, the Principal Components (PCs), which are uncorrelated and ordered so that the first few retain most of the variation present in all of the original

variables. Computation of the PCs reduces to the solution of an eigenvalue problem for a positive semi-definite symmetric matrix. Thus, the definition and computation of PCs are straightforward, but this simple technique has a wide variety of different applications, as well as a number of different derivations [20]. There are two popular algorithms for applying PCA; Singular Value Decomposition (SVD) and Eigenvalue Decomposition (EVD). In this research, SVD was applied since it is more robust when matrices are numerically singular or very near to singular [21].

If a data has "n" observations and "m" features, a matrix, X, of $(n \times m)$ dimensions is generated and the SVD can be defined as:

$$X = USV^T \tag{1}$$

where U is an $(n \times r)$ orthogonal matrix, S is a $(r \times r)$ diagonal matrix that contains the variations of principal components (PCs) and are arranged in the diagonal according to the rank, r, and V is an $(m \times r)$ orthogonal matrix contains PCs which denoted as loadings. The importance of the SVD for PCA is twofold. Firstly, it provides a computationally efficient method of actually finding PCs. It is clear that if U, S, V satisfying Eq. (1), then V and S will give the eigenvectors and the square roots of the eigenvalues of XTX, and hence the coefficients and standard deviations of the PCs. To see scaled versions of PC scores in U, multiply eq. (1) by V to give:

$$XV = USV^TV = US, \text{ and } V^TV = I_r \tag{2}$$

where XV is a (n × r) matrix whose k^{th} column (K=1, 2…, m) consists of the PC scores for the k^{th} PC; I_r is an (r × r) identity matrix. A second virtue of the SVD is that it provides additional insight into what a PCA actually does, and it gives useful means, both graphical and algebraic, of representing the results of a PCA. Furthermore, the SVD is useful in terms of both computation and interpretation in PC regression and in examining the links between PCA and correspondence analysis.

3. Experimental setup

Due to operating conditions and the nature of process fluids passing through mechanical components (e.g. impellers, fans, screws) of rotating machines (e.g. pumps, cooling towers, compressors), faults like rotor unbalance due to wear, belt damage due to tension, and pulleys misalignment due to looseness may be initiated. The main objective of the test rig used in this research is to simulate common faults in rotary machines installed in many industries. It was constructed from two shafts supported on four bearings of UCP206 bearing type as shown in Figure 1. The power is transmitted to the second shaft through pulleys and belt and each shaft carries one disc. A three phase servo motor of APM-SE09MEK model type with a permanent connected short shaft was used as a power source and its speed was controlled by a servo drive of L7SA020A model type. Both of the motor and drive were produced by LS Group (South Korean Corporation). The motor shaft was connected to a flexible coupling that assembled the motor shaft and the first shaft in the test rig.

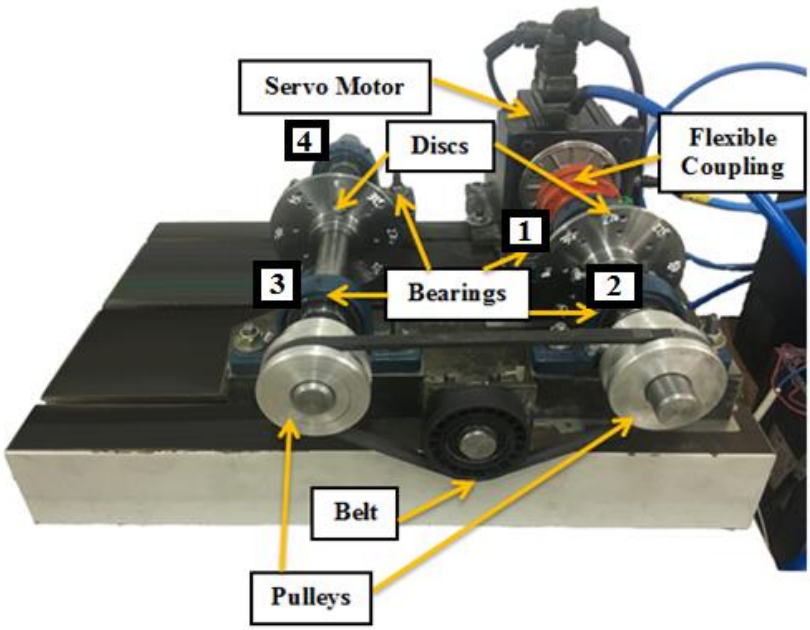

Figure 1: Test rig.

Measurements were recorded at steady-state condition and datasets of 78 cases were collected for healthy and different fault cases. The faults applied to the test rig are static unbalance, dynamic unbalance, pulley misalignment, belt damage, and combined faults as arranged in Table 1. The static unbalance was modeled as one weighted mass installed in the rotors of two shafts. The dynamic unbalance was modeled as two weighted masses the angle between was slightly loosened to simulate the belt damage faults. Combined faults cases were simulated by testing the rig with two faults at the same time (unbalance with pulley misalignment and unbalance with belt damage). Each fault case was tested at 1000 rpm (16.67 Hz), 1500 rpm (25 Hz), and 2000 rpm (33.33 Hz) to study the ability of distinguishing different faults in variable speed machines.

Table 1: Description for different fault cases.

Symbol	Description
C0	Healthy condition
C1	Static unbalance on one shaft
C2	Static unbalance on two shafts
C3	Dynamic unbalance
C4	Pulley misalignment
C5	Combined unbalance and pulley misalignment
C6	Belt damage
C7	Combined unbalance and belt damage

4. Instrumentation

A data acquisition system was used to record the data measured by sensors which converted from analog to digital form at a certain sampling rate. B&K PULSE input module type 3050-A-060 has been used as a data acquisition system in this analysis. It includes six high-precision input channels with an input range from DC to 51.2 kHz. A standard LAN cable was used for synchronous sampling between the module and system power. The module allows front panels to be interchanged freely, with a variety of connectors for

different transducers and applications. Electronic data sheet (TEDS) transducers were connected to the module which allowing automatic front-end and analyzer setup based on TEDS information stored in the transducer such as family, serial number, sensitivity, and manufacturer. Two TEDS transducers were connected to the first two channels of the module and each transducer was connected to the module by a Bayonet Neill–Concelman (BNC) cable of radio frequency coaxial connector. The two transducers were used to record the vibration measurements in the vertical and horizontal directions at the same time on the same bearing.

Pulse Labshop software was setup and vibration signals were collected through a frequency range from 0 to 400 Hz and time wave forms were sampled to 4096 samples to record 4sec (1024 samples/s) and to satisfy Nyquist–Shannon sampling theorem. FFT spectra have 1600 lines of resolution yielding a frequency resolution of 0.25 Hz. On the other hand, the servo motor of APM-SE09MEK model type was connected to APD-L7S servo drive as shown in Figure 2 for complete control on input and output parameters of motor.

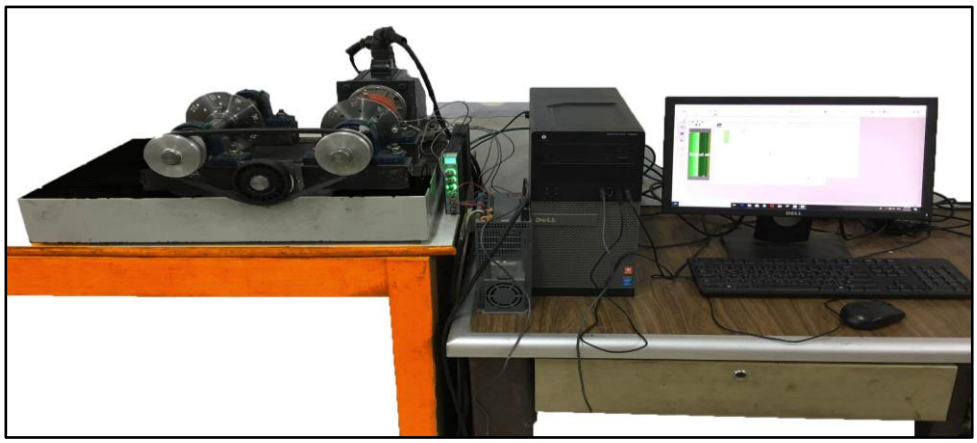

Figure 2: Configuration of data collection system.

5. Results

5.1 Vibration dataset

FFT was computed for vibration signals and the RMS at bearing No. 1 and 2 (bearings which support the shaft coupled with motor) in the horizontal (Ht) and vertical (Vt) direction was estimated. The vibration analysis was performed on the frequency spectrum and time wave form as displayed in the example shown in Figure 3. This figure presents the effect of unbalance fault on the vibration pattern and level since the unbalance increased the amplitudes at 2X which considered the dominant to increase the RMS of time signal. The effects of different faults on changing the values of 1X, 2X, 3X, and RMS levels are shown in Figure 4 to Figure 7. The features values of these figures are arranged in Table 2. The correlated features were estimated using the following formula:

$$\text{Correlated features} = \frac{N_{corr}}{16} \times 100\ (\%) \qquad (3)$$

where N_{corr} is the number of correlated features in one case. It was observed that the highly correlated features have been investigated by static unbalance on one shaft (C1) and belt damage case (C6) followed by healthy (C0), dynamic unbalance (C3), pulley misalignment (C4), and combined faults (C7 and C5). The numbers of correlated features have a ratio of 62.5, 62.5, 56.25, 43.75, 37.5, 37.5, and 25% of total features, respectively. On the other hand, all the features of static unbalance on two shafts case (C2) are uncorrelated. However there is an observed change in the levels of the selected vibration features, it is not adequate for the diagnosis of some simulated faults without other aided tools [22], [23]. In the next

section, one of the aided tools (PCA) is employed to identify and distinguish the faults which have correlated vibration features since PCA retrieves as much as possible the variations in these features in the form of uncorrelated PCs.

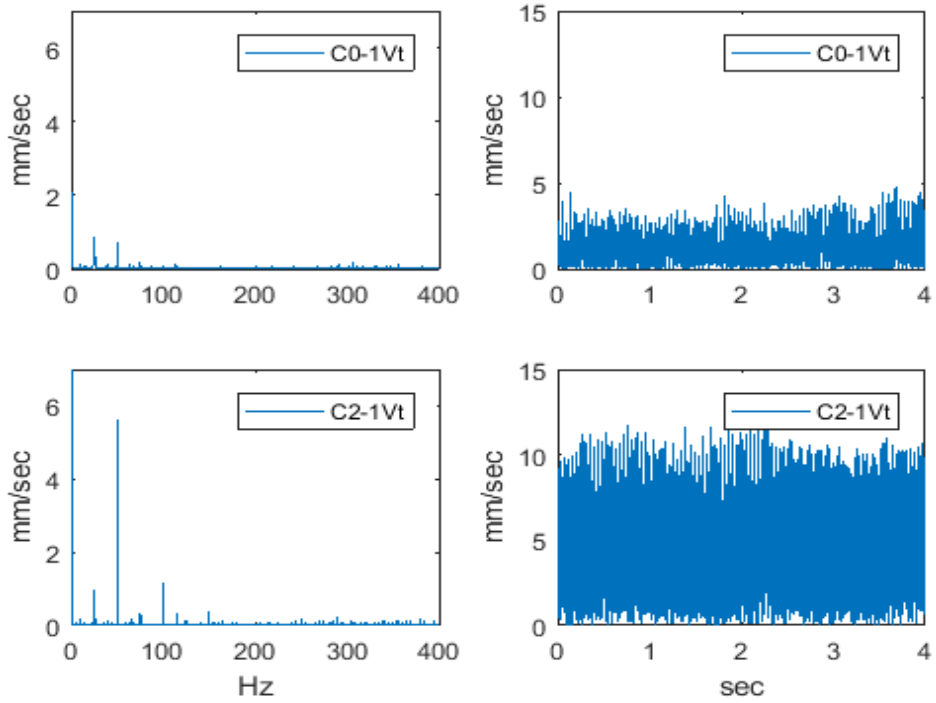

Figure 3: Vibration measurements for healthy and unbalance cases -1500rpm (25Hz) - Bearing No. (1)-vertical direction.

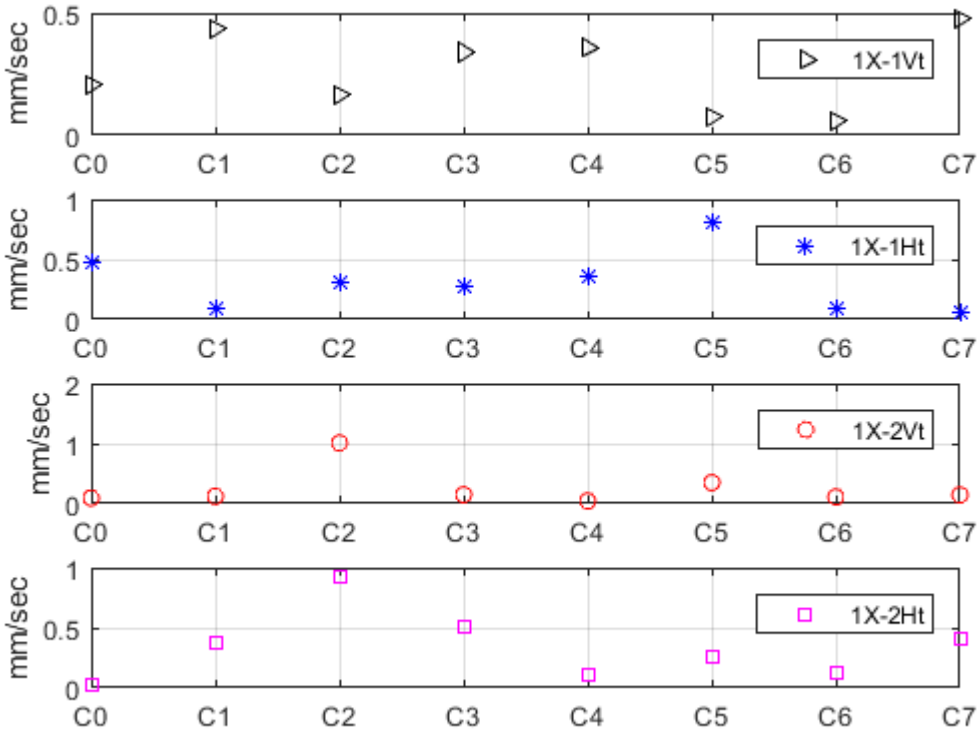

Figure 4: Variation of 1X for radial directions of two bearings.

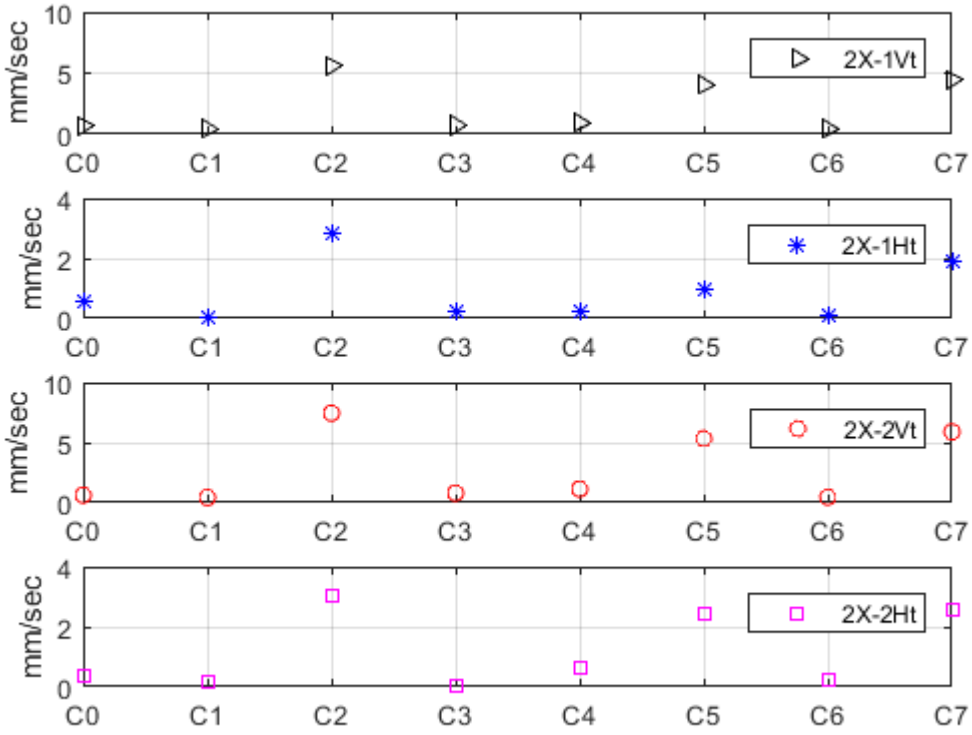

Figure 5: Variation of 2X for radial directions of two bearings.

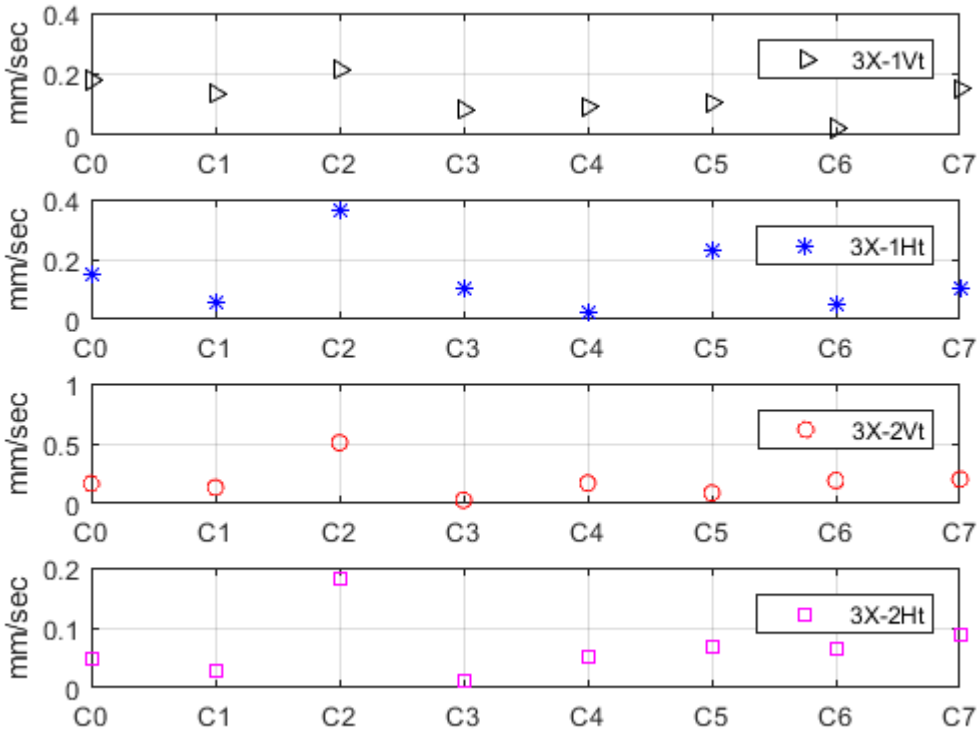

Figure 6: Variation of 3X for radial directions of two bearings.

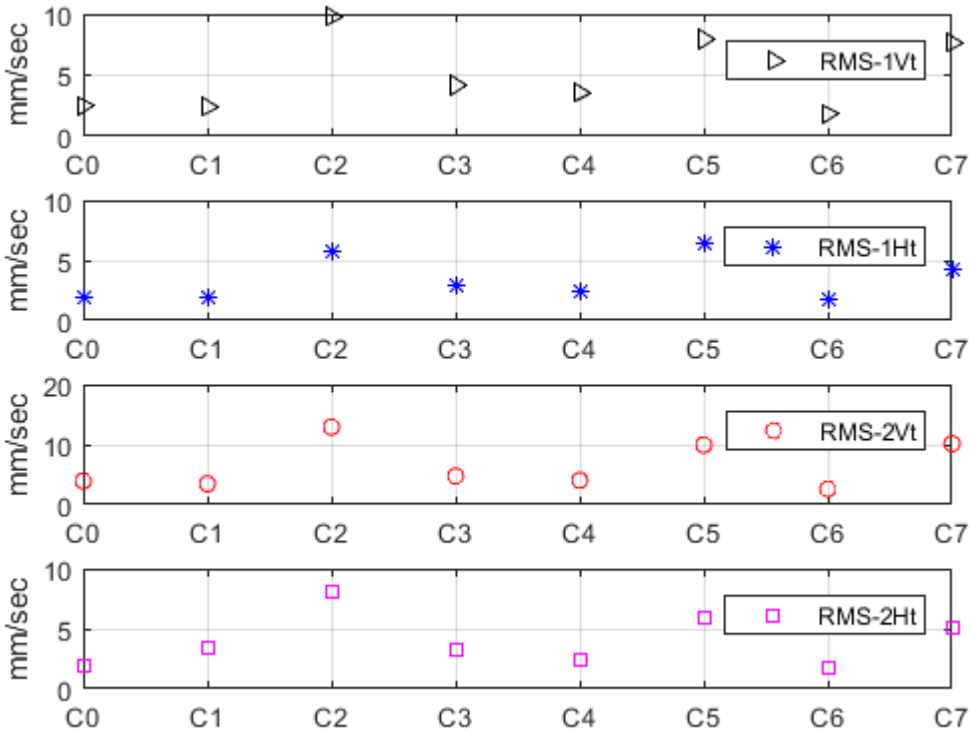

Figure 7: Variation of RMS for radial directions of two bearing.

Table 2: Vibration features for healthy and different faulty cases.

Features	C0	C1	C2	C3	C4	C5	C6	C7
1X-1Vt (mm/s)	0.21	0.43	0.17	0.34	0.36	0.07	0.06	0.48
1X-1Ht (mm/s)	0.47	0.10	0.31	0.27	0.35	0.81	0.10	0.07
1X-2Vt (mm/s)	0.10	0.12	1.01	0.15	0.05	0.35	0.11	0.15
1X-2Ht (mm/s)	0.03	0.38	0.93	0.51	0.11	0.26	0.12	0.41
2X-1Vt (mm/s)	0.70	0.45	5.63	0.74	0.94	4.04	0.46	4.47
2X-1Ht (mm/s)	0.55	0.03	2.85	0.26	0.22	0.96	0.10	1.92
2X-2Vt (mm/s)	0.63	0.43	7.45	0.81	1.15	5.33	0.47	5.90
2X-2Ht (mm/s)	0.40	0.15	3.07	0.07	0.65	2.40	0.26	2.59
3X-1Vt (mm/s)	0.18	0.14	0.22	0.08	0.09	0.11	0.02	0.15
3X-1Ht (mm/s)	0.15	0.06	0.37	0.10	0.03	0.23	0.05	0.11
3X-2Vt (mm/s)	0.17	0.13	0.51	0.03	0.17	0.09	0.19	0.20
3X-2Ht (mm/s)	0.05	0.03	0.18	0.01	0.05	0.07	0.07	0.09
RMS-1Vt (mm/s)	2.51	2.40	9.78	4.19	3.58	7.95	1.84	7.64
RMS-1Ht (mm/s)	1.86	1.94	5.71	2.87	2.37	6.38	1.77	4.18
RMS-2Vt (mm/s)	3.96	3.49	12.92	4.76	4.06	9.96	2.65	10.17
RMS-2Ht (mm/s)	1.93	3.44	8.08	3.18	2.33	5.98	1.79	5.05
Correlated Features (%)	56.25	62.5	0	43.75	37.5	25	62.5	37.5

	1st Correlated features in one row		2nd Correlated features in one row		3rd Correlated features in one row

5.2 Principal Component Analysis

PCA was applied to extract the PCs of healthy and different fault cases. The four features in each direction of two bearings were arranged in a matrix of (78 × 16) which represents 78 observations and 16 features in each observation (4 features for each direction × 2 bearings × 2 directions). The variation of PCs is the main parameter that describes which PC included the most features since the greater the variation of PCs the more features extracted. The variation of PCs is displayed in Figure 8. Since the first and second PCs have the largest variation compared to other PCs, they only were considered in this analysis. The features of PC1 and PC2 are shown in Figure 9 and arranged in Table 3. It was found that all correlated vibration features are converted into uncorrelated PCs for all cases except the correlated PC1 between healthy (C0) and static unbalance on one shaft (C1). These uncorrelated PCs aid to solve the issue of good identification for different cases.

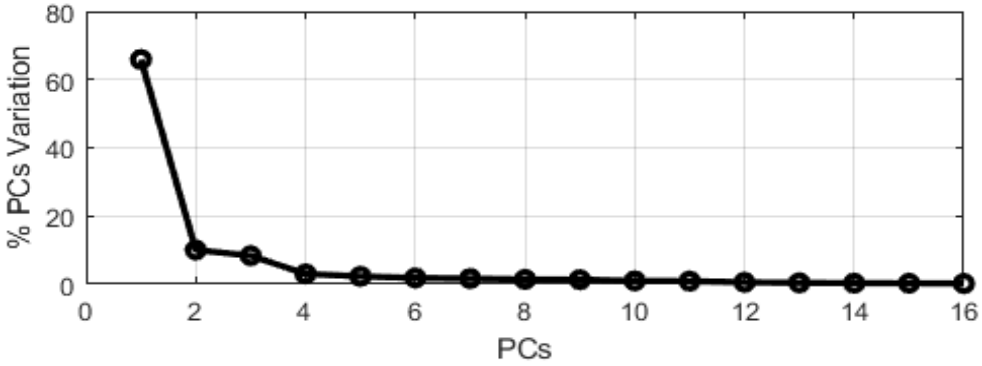

Figure 8: PCs variation.

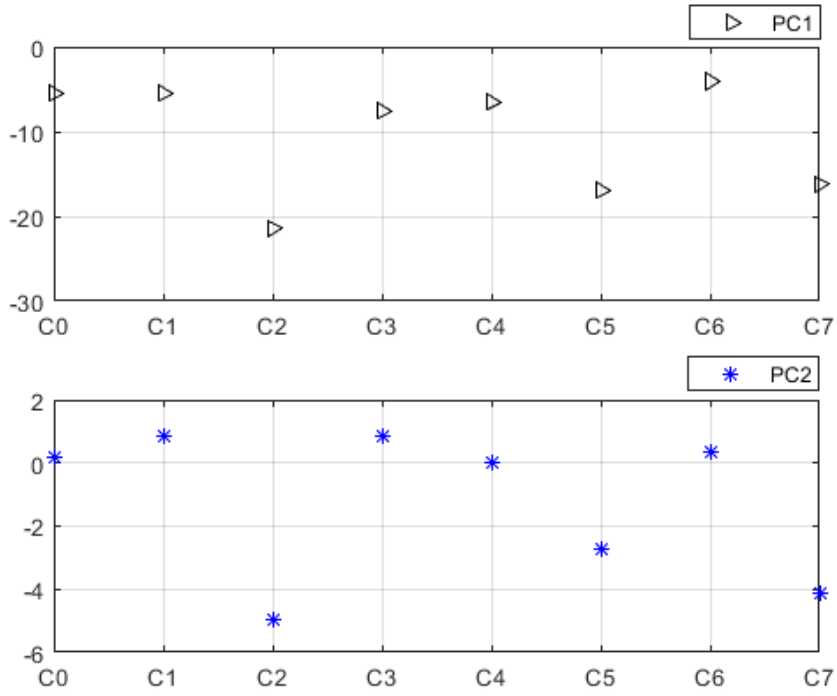

Figure 9: PC1 and PC2 for healthy and different fault cases.

Table 3: PC1 and PC2 for healthy and different faulty cases.

	C0	C1	C2	C3	C4	C5	C6	C7
PC1	-5.45	-5.46	-21.38	-7.51	-6.50	-16.88	-4.04	-16.22
PC2	0.16	0.87	-4.98	0.87	0.01	-2.72	0.35	-4.11

6. Conclusions

Condition monitoring based on vibration signatures and PCA has been presented in this paper. PCA was applied to reduce the dimensionality and correlated features and improve the accuracy of fault diagnosis process. Vibration signals were measured for healthy and different faulty cases such as unbalance, pulley misalignment, belt damage, and combined faults. After that, the features of these signals were extracted. It was found that the highly correlated features have been investigated by static unbalance on one shaft (C1) and belt damage case (C6) followed by healthy (C0), dynamic unbalance (C3), pulley misalignment (C4), and combined faults (C7 and C5). The numbers of correlated features have a ratio of 62.5, 62.5, 56.25, 43.75, 37.5, 37.5, and 25% of total features, respectively. On the other hand, all the features of static unbalance on two shafts case (C2) are uncorrelated. To improve the issue of correlated features, PCA method was implemented using vibration features as input parameters to the PCA model. It was concluded that all correlated vibration features are converted into uncorrelated PCs for all cases except the correlated PC1 between healthy (C0) and static unbalance on one shaft (C1). This means that PCA has the superior to identify and distinguish different cases which have an ambiguous diagnosis when using conventional vibration measurements.

References

[1] N. Verma, T. Subramanian, Cost benefit analysis of intelligent condition based maintenance of rotating machinery, 7th IEEE Conference on Industrial Electronics and Applications (ICIEA) (2012), pp. 1390-1394.

[2] Z. Zhang, Data mining approaches for intelligent condition-based maintenance, a framework of intelligent fault diagnosis and prognosis System (IFDPS) (2014).

[3] S. Shao, W. Sun, P. Wang, R. Gao, R. Yan, Learning features from vibration signals for induction motor fault diagnosis, International Symposium on Flexible Automation (ISFA) IEEE (2016), pp. 71-76.

[4] O. Abdeljaber, O. Avci, S. Kiranyaz, M. Gabbouj, D. Inman, Real-time vibration-based structural damage detection using one-dimensional convolutional neural networks, Journal of Sound and Vibration (2017), vol. 388, pp. 154-170.

[5] Z. Li, J. Chen,Y. Zi, J. Pan, Independence-oriented VMD to identify fault feature for wheel set bearing fault diagnosis of high speed locomotive, Mechanical Systems and Signal Processing (2017), vol. 85, pp. 512-529.

[6] Y. Lei, Z. Qiao, X. Xu, J. Lin, S. Niu, An underdamped stochastic resonance method with stable-state matching for incipient fault diagnosis of rolling element bearings, Mechanical Systems and Signal Processing (2017), vol. 94, pp. 148-164.

[7] Z. Huo, Y. Zhang, P. Francq, L. Shu, J. Huang, Incipient fault diagnosis of roller bearing using optimized wavelet transform based multi-speed vibration signatures, IEEE Access (2017).

[8] D. Susilo, A. Widodo,T. Prahasto, M. Nizam, Fault diagnosis of roller bearing using parameter evaluation technique and multi-class support vector machine, AIP Conference Proceedings (2017), vol. 1788, no. 1, p. 030081.

[9] M. Islam, J. Kim, S. Khan, J. Kim, Reliable bearing fault diagnosis using Bayesian inference-based multi-class support vector machines, The Journal of the Acoustical Society of America (2017), vol. 141(2), pp. 89-95.

[10] Y. Lei, Z. Liu, J. Ouazri, J. Lin, A fault diagnosis method of rolling element bearings based on CEEMDAN, Journal of Mechanical Engineering Science (2017), vol. 231(10), pp. 1804-1815.

[11] H. Ahmed, M. Wong, A. Nandi, Intelligent condition monitoring method for bearing faults from highly compressed measurements using sparse over-complete features, Mechanical Systems and Signal Processing (2018), vol. 99, pp. 459-477.
[12] B. Yang, T. Han, Z. Yin, Fault diagnosis system of induction motors using feature extraction, feature selection and classification algorithm, JSME International Journal Series C Mechanical Systems, Machine Elements and Manufacturing (2006), vol. 49(3), pp. 734-741
[13] M. Farajzadeh, R. Razavi, M. Saif, Dimensionality reduction-based diagnosis of bearing defects in induction motors, IEEE International Conference on Systems, Man, and Cybernetics (SMC) (2017), pp. 2539–2544.
[14] J. Saucedo, M. Delgado, R. Osornio, R. De Jesus, Multifault diagnosis method applied to an electric machine based on high-dimensional feature reduction, IEEE Transactions on industry applications (2017), vol. 53(3), pp. 3086-3097.
[15] T. Plante, L. Stanley, A. Nejadpak, C. Yang, Rotating machine fault detection using principal component analysis of vibration signal, IEEE autotestcon (2016),pp. 1-7.
[16] K. Sarita, R. Devarapalli, S. Kumar, H. Malik, F. Márquez, P. Rai, Principal component analysis technique for early fault detection, Journal of Intelligent & Fuzzy Systems (2021), PP. 1-12.
[17] Y. Yuan, C. Chen, Fault detection of rolling bearing based on principal component analysis and empirical mode decomposition, AIMS Mathematics (2020), vol. 5(6), pp. 5916-5938.
[18] R. Teti, K. Jemielniak, G. Donnell, D. Dornfeld, Advanced monitoring of machining operations, CIRP annals (2010), vol. 59(2), pp. 717-739
[19] T. Sutharssan, S. Stoyanov, C. Bailey, C. Yin, Prognostic and health management for engineering systems: a review of the data-driven approach and algorithms, The Journal of engineering (2015), vol. 7, pp. 215-222
[20] I. Jolliffe, Principal component analysis, Springer (2010).
[21] A. Stief, J. Ottewill, J. Baranowski, M. Orkisz, A PCA-two stage Bayesian sensor fusion approach for diagnosing electrical and mechanical faults in induction motors, IEEE Transactions on Industrial Electronics (2019).
[22] J. Sinou, Experimental response and vibrational characteristics of a slotted rotor, Communications in Nonlinear Science and Numerical Simulation (2009), vol. 14(7), pp. 3179-3194.
[23] J. Sinha, Health monitoring techniques for rotating machinery, PhD University of Wales Swansea (2002).